Received: 19 July 2018 | Revised: 9 November 2018 | Accepted: 13 November 2018

DOI: 10.1111/fwb.13240

ORIGINAL ARTICLE

WILEY Freshwater Biology

Spatial heterogeneity and short-term oxygen dynamics in the rhizosphere of *Vallisneria spiralis*: Implications for nutrient cycling

Ugo Marzocchi[1] | Sara Benelli[2] | Morten Larsen[1] | Marco Bartoli[3,4] | Ronnie N. Glud[1,5]

[1]Department of Biology and Nordic Center for Earth Evolution, University of Southern Denmark, Odense, Denmark

[2]Department of Life Sciences and Biotechnology, University of Ferrara, Ferrara, Italy

[3]Department of Chemistry, Life Sciences and Environmental Sustainability, University of Parma, Parma, Italy

[4]Marine Research Institute, University of Klaipeda, Klaipeda, Lithuania

[5]Department of Ocean and Environmental Sciences, Tokyo University of Marine Science and Technology, Tokyo, Japan

Correspondence
Ugo Marzocchi, Department of Bioscience, Center for Electromicrobiology, Aarhus, Denmark.
Email: ugo.marzocchi@bios.au.dk

Funding information
Danish National Research Council, Grant/Award Number: 0602-02276B and 12-125843; Villum Fonden, Grant/Award Number: 13881; H2020 European Research Council, Grant/Award Number: 669947

Abstract

1. Aquatic macrophytes modify the sediment biogeochemistry via radial oxygen loss (ROL) from their roots. However, the variation in ROL and its implication for nutrient availability remains poorly explored.
2. Here, we use planar O_2 optodes to investigate the spatial heterogeneity of oxic niches within the rhizosphere of *Vallisneria spiralis* and their alteration following variable light and ambient O_2 levels. The effect of ROL on NH_4^+ and PO_4^{3-} distribution in the rhizosphere was evaluated by a combination of ^{15}N isotopic techniques, 2D sampling, and electron microscopy.
3. A single specimen of *V. spiralis* could maintain an oxidised sediment volume of 41–47 cm^3 and 10–27 cm^3 in the rhizosphere at 100% and 38% dissolved oxygen saturation in the overlying water, respectively. Whatever the environmental conditions, the ROL was, however, very heterogeneous and dependent on root age and architecture of the root system.
4. ROL stimulated the coupling between denitrification and nitrification in the sediment both under dark (+25 μmol N-N_2 m^{-2} hr^{-1}) and light (+70 μmol N-N_2 m^{-2} hr^{-1}) conditions. This, in combination with plant uptake, contributed to intense removal of NH_4^+ from the pore water. Similarly, PO_4^{3-} was highly depleted in the rhizosphere. The detection of Fe-P plaques on the roots surface indicated substantial entrapment of P as a consequence of ROL.
5. The extensive spatio-temporal heterogeneity of oxic and anoxic conditions ensured that aerobic and anaerobic processes co-occurred in the rhizosphere and this presumably reduced potential nutrient limitation while maximising plant fitness in an otherwise hostile reduced environment.

KEYWORDS
nitrogen, phosphorous, planar oxygen optode, radial oxygen loss, rhizosphere

1 | INTRODUCTION

Submerged aquatic macrophytes can transport variable amount of O_2 to the roots to allow their respiration in waterlogged soils (Armstrong, 1979). Such transport primarily occurs through the aerenchyma that consists of air canals connecting leaves, stems and roots (Colmer, 2003b; Smirnoff & Crawford, 1983). The development of an aerenchyma is presumably an adaptation of submerged macrophytes to live within sediments that are strictly anoxic a few millimetres from the surface (Colmer, 2003b; Longhi,

Bartoli, Nizzoli, & Viaroli, 2013). Part of the transported O_2 may leak out and create oxidised sediment layers around the roots (Laskov, Horn, & Hupfer, 2006). In seagrasses such as *Zoostera marina* and *Ruppia maritima*, radial oxygen loss (ROL) may occur only in the proximity of the root tips (e.g. Jensen, Kuhl, Glud, Jorgensen, & Prieme, 2005; Jovanovic, Pedersen, Larsen, Kristensen, & Glud, 2015). In other plants, such as *Potamogeton perfoliatus*, the whole rhizosphere displays ROL, suggesting that the whole root length is permeable to O_2 (Caffrey & Kemp, 1991). Whereas the onset of diffusion barriers at the root basal region allows to maximise longitudinal O_2 transport to the actively growing root apex (Colmer, 2003a), maintaining high permeability throughout the rhizosphere appears to be a strategy for optimising nutrient uptake and maintaining positive redox conditions (e.g. Mei, Yang, Tam, Wang, & Li, 2014).

While O_2 transport via the aerenchyma is necessary to sustain the aerobic metabolism of the roots living in an otherwise anoxic environment, the leakage of O_2 to the surrounding sediments has several secondary implications. Radial oxygen loss can effectively oxidise reduced toxic compounds (i.e. free sulfides and metal ions) around and within the roots, where they otherwise may induce physiological stress and damage to the plant (Geurts et al., 2009; Koch & Mendelssohn, 1989). In addition, ROL may promote aerobic microbial processes that mobilise nutrients and trace-elements from recalcitrant organic matter (Harvey, Tuttle, & Bell, 1995; Magri et al., 2018) or, on the contrary, favour nutrient immobilisation (e.g. phosphorous and iron) via adsorption or precipitation (e.g. Christensen, Jensen, Andersen, Wigand, & Holmer, 1998; Povidisa, Delefosse, & Holmer, 2009; St-Cyr, Fortin, & Campbell, 1993). Implications for nutrient mobility and turnover are expected to vary largely among different submerged macrophytes depending on ROL intensity, distribution along the roots, and temporal dynamics. In freshwater bodies, the same macrophyte species can be found across gradients of nutrients availability, water flow regimes, and water oxic level, which may vary from normoxic to suboxic levels on a daily basis. Especially eutrophic environments may display pronounced short-term variation in ambient O_2 levels, but for many species the implications for the ROL is unknown. This is relevant as hypoxic events are a menace for macrophytes due to limited capacity of sediment to re-oxidise the products of anaerobic microbial metabolisms, leading to chemically reduced conditions and the build-up of phytotoxic compounds. The plasticity of macrophytes and their capacity to vary the O_2 transport via ROL may determine their resilience in dynamic settings and provide a competitive advantage for the colonisation of sediments with different organic content.

A large body of work has been conducted to explore the implications of ROL from the widely distributed freshwater macrophyte *Vallisneria spiralis*. Oxygen transport to sediments by *V. spiralis* was firstly indirectly inferred from an imbalance in the benthic O_2 and total inorganic carbon fluxes measured in the light in muddy vegetated sediments (Pinardi et al., 2009; Ribaudo, Bartoli, Racchetti, Longhi, & Viaroli, 2011). Based on the same approach, Soana and Bartoli (2013) demonstrated how *V. spiralis* varies the O_2 delivered to the sediment seasonally, depending upon the pore water redox conditions, with highest delivery of O_2 in the late summer coinciding with the more reduced chemical conditions. The lower concentration of CH_4 and metal ions (Fe^{2+} and Mn^{2+}) and the stimulated coupling between denitrification and nitrification in vegetated versus non-vegetated sediments further supported the hypothesis of rhizosphere-driven sediment oxygenation (Racchetti, Longhi, Ribaudo, Soana, & Bartoli, 2017; Racchetti et al., 2010; Ribaudo et al., 2011; Soana et al., 2015). Whereas the above-mentioned studies provide indirect evidence of O_2 leakage from roots, direct measurement of ROL in *V. spiralis* was only recently shown via planar optode application (Han, Ren, Tang, Xu, & Xie, 2016; Han et al., 2018). These studies demonstrated O_2 leakage of the roots, analysed the effect of irradiance on ROL, and showed a link between ROL and the immobilisation of porewater P.

In this work, we explored the fine-scale O_2 dynamics in the rhizosphere of *V. spiralis* by comparatively analysing the effects of the ambient O_2 concentration and of photosynthesis on ROL. Moreover, we further investigated the link between O_2 dynamics for nitrogen and phosphorous cycling in the rhizosphere by analysing the effect of light and dark cycles on the coupled denitrification and nitrification activity, and the formation of Fe-P plaques on the surface of roots of different age. The overall effect of the rhizosphere on nitrogen and phosphorous concentration and distribution was assessed via 2D sampling techniques integrating a 2-week period.

2 | METHODS

2.1 | Sediment, plant sampling and pre-incubation

In May 2015, shoots of *V. spiralis*, sediment, and water (200 L) were collected at 1m depth in the Mincio River in Massimbona (northern Italy). Single specimens of *V. spiralis* were extracted by hand from the sediment to minimise root damage. Sediment was sampled from unvegetated banks in proximity of the *V. spiralis* meadow using acrylic liners (inner diameter × length: 8 × 40 cm). Within a few hours, samples were brought to the laboratory and stored in a temperature-controlled room at 20°C ± 2 to resemble in situ temperature typical for the season (Pinardi et al., 2009). Sediment was homogenised and sieved (mesh size 0.5 mm) to exclude macroinvertebrates, stones, and other irregularities, before being packed into four acrylic rhizotrons (H × W × D: 41 × 20 × 3 cm.) to about half of the volume. A shoot of *V. spiralis* was then transplanted into each rhizotron and the rest of the volume was filled with in situ water. An optode foil pre-installed on the inner wall of each rhizotron allowed for later oxygen imaging. The rhizotrons were placed into a large tank (100 L) containing in situ water and tilted of 45° (optode wall face-down) to facilitate root growth along the optode foil (see below). Water in the tank and in the rhizotrons was kept mixed by submersible pumps and flushed with air. Plants were illuminated on a 13:11 hr light/dark cycle using LED lights positioned above the aquarium. Irradiance during light phases was set to 200 μmol photons m^{-2} s^{-1} to match the daily average light levels at the sampling site and to ensure photosynthesis light-saturation (Bartoli unpublished results). Plants were

pre-incubated for 14 days to assure plant acclimation to the experimental conditions before the experiments started.

2.2 | Effect of ambient water O_2 level on ROL

After the acclimation phase, one rhizotron that showed root grown along the planar optode wall was extracted from the reservoir and positioned in front of the camera and LED setup for planar optode imaging (Figure S1). The experiment consisted of two phases: (a) a growth phase, characterised by continued expansion of the oxic area of the rhizosphere; and (b) a steady-state phase when plant growth ceased. During the growth phase, we comparatively analysed the extent of the ROL induced-oxic area around new, growing roots and old, not growing roots during light and dark conditions. The steady-state phase was used to assess the effect of dissolved oxygen saturation (100, 38, and 70%) on the ROL intensity, O_2 distribution and dynamics in the rhizosphere, both under light and dark conditions. Extent of the oxic area around single roots and the overall oxic area of the rhizosphere were measured by processing planar optode images via the software ImageJ (http://imagej.nih.gov). ROL intensity was estimated as described below.

Oxygen levels in the water overlying the sediment were regulated by mixing air and N_2 via mass flow controllers (5850 S, Brooks Instruments, USA) controlled by a digital control/readout unit (type 0154, Brooks Instrument, USA). The O_2 levels and the temperature of the water were monitored throughout the experiment via a fibre-optic O_2 sensor and a thermometer connected to an oxygen meter (FireStingO_2, PyroScience, Germany). Planar optode images were acquired every 20 min. Image acquisition proceeded throughout at least one light/dark cycle (i.e. 24 hr), while the overlying water O_2 level was kept constant. At the end of each O_2 treatment, the overlying water was replaced with fresh in situ water to avoid nutrient depletion and accumulation of waste products from the plant metabolism and sediment processes. Overall, images were recorded over 24 hr for the growth phase and 130 hr for the steady-state phase.

2.3 | Oxygen imaging principle and optode sensor fabrication

The basic optode set up resembles the original description (Glud, Ramsing, Gundersen, & Klimant, 1996) but here we applied the colour ratiometric sensing approach (Larsen, Borisov, Grunwald, Klimant, & Glud, 2011). The procedure is based on the relative change in intensity of O_2 sensitive red emission light versus the O_2 insensitive green emission light (Larsen et al., 2011). The O_2 images were recorded using a digital single lens reflex camera (Canon EOS 1000D) equipped with a 530 nm long-pass filter (Edmund Optics). Excitation light was delivered from seven high-power LEDs (λ peak = 447.5 nm; SR-02-R0500, Luxeon Star LEDs) equipped with a 470-nm short-pass filter (Edmund Optics). The O_2 planar optode sensor applied in this study was fabricated as in Larsen et al. (2011). The applied O_2 optodes had an O_2 sensitive layer of <2 μm that was coated by a 15 μm semi-transparent silicone layer with 1% (wt/wt) carbon powder. The coating ensured that any structures behind the sensor foil remained visible during O_2 measurements, without affecting the ratiometric approach (Larsen et al., 2011). The size of the optode foils was 23 × 17 cm. The excitation light was trigged and synchronised with the camera via a control unit (LED trigger light; Fish 'n' chips, Germany). Excitation light and image acquisition settings were regulated using the software Look@RGB (available at http://www.fish-n-chips.de/Look@RGB/publish.htm).

2.4 | Images calibration

For calibration of the O_2 sensor, we used the luminescent intensity ratio (R) of the green and red images recorded simultaneously by the camera, according to Larsen et al. (2011):

$$R = \frac{\text{Red} - \text{Green}}{\text{Green}} \quad (1)$$

where Red and Green are the pixel intensities of the red and green images, respectively.

A modified Stern–Volmer equation adequately describes the response of the sensor (Klimant, Meyer, & Kuhl, 1995):

$$\frac{R}{R_0} = \left[\alpha + (1-\alpha)\left(\frac{1}{1+K_{sv}+C}\right)\right] \quad (2)$$

where α is the non-quenchable fraction of the luminescence signal, K_{sv} the Stern–Volmer quenching constant, R the (red-green)/green luminescent intensity ratio, R_0 is the luminescent intensity ratio in the absence of O_2, and C is the O_2 concentration. Values for α and K_{sv} were determined by curve fitting the variation in R/R_0 as a function of O_2 concentration. Finally, O_2 concentration can be calculated for each image pixel by rearranging Equation 2 as follows:

$$C = \frac{R_0 - R}{K_{sv}(R - R_0\alpha)} \quad (3)$$

with R_0 determined in the anoxic sediment.

2.5 | Estimation of sediment respiration and ROL

The areal O_2 consumption at the sediment-water interface (R_{SWI}) was calculated from microscale O_2 depth-profiles at the sediment-water interface, extracted from planar optode images and modelled with the algorithm developed by Berg, Risgaard-Petersen, and Rysgaard (1998). Due to the higher concentration of reduced species at depth, the O_2 respiration in proximity of the roots (R_S) can be higher than at sediment-water interface (R_{SWI}). R_S was calculated as described above for R_{SWI}, but from depth-profiles measured right after the sediment was mixed and packed into the rhizotrons. Volume specific R_S was calculated from the areal consumption divided by the O_2 penetration depth. The oxygen diffusion coefficient (Ds) was calculated according to Ullman and Aller (1982) from the sediment porosity and diffusion coefficient in water. The diffusion coefficient in water was calculated as in (Boudreau, 1997) as a function of temperature and

salinity, while the porosity was determined from sediment density and water content measured as described in (Dalsgaard et al., 2000).

The detection limit of the optode was quantified as three times the standard deviation of the measured concentration at anoxia for an area of 5 × 5 cm and amounted to 2 μmol/l (about 1% air saturation). thus, oxic areas were defined as values with a measured O_2 concentration above 2 μmol/l. the spatial resolution achieved by the optode system was 210 μm/pixel.

The ROL per area of root surface was estimated with the equation for radial diffusion proposed by Fenchel (1996):

$$\mathrm{ROL} = \varphi \times R_s x L \times \left(\frac{L}{2A} + 1\right) \quad (4)$$

where φ is the sediment porosity, R_S is the respiration of the sediment, L (mm) is half the width of the oxygenated zone measured at the planar optode wall, and A (mm) is half the width of the root diameter. Since planar optode measurements were performed along a wall not consuming O_2, the measured extent of the oxic area around a single root was larger compared to a root surrounded by sediment only (Glud, 2008; Meysman, Galaktionov, Glud, & Middelburg, 2010; Wenzhöfer & Glud, 2004). Assuming that the oxic area around a root in contact with the planar optode can be approximated as a half-cylinder, and that the oxic volume around the roots is independent of the presence of a wall, the *true* radial O_2 distribution around a root surrounded by sediment can be calculated as in (Frederiksen & Glud, 2006). The total O_2 transport into the rhizosphere by ROL at steady-state was calculated from the oxic volume of the rhizosphere multiplied by the respiration of the sediment (Rs). The oxic volume of the whole rhizosphere was calculated from the oxic area on the planar optode wall assuming hemispherical geometry (Frederiksen & Glud, 2006).

2.6 | Coupled denitrification and nitrification rates in vegetated and unvegetated sediment

To investigate the influence of ROL and its diel variation on the coupling between nitrification and denitrification in the sediment at the rhizosphere, an additional number of *V. spiralis* shoots and about 20 L of sediment was collected along with the samples for ROL studies as described above. In the laboratory, the sediment was homogenised and transferred into cylindrical acrylic microcosms (inner diameter × length: 7.5 × 10 cm, n = 12) and in the half of the microcosms two specimens of *V. spiralis* were added, simulating in situ plant density. Each microcosm was provided with four series of vertical holes, spaced at 1 cm and filled with silicon glue. Plants were let acclimatise for 3 weeks in a tank with in situ water (renewed every 2 days) and exposed to 13:11 light:dark cycle (irradiance of 200 µmol photons m^{-2} s^{-1}). After the acclimation period, light and dark incubations were performed as described in Soana et al. (2015). Briefly, an anoxic $^{15}NH_4^+$ solution (10 mM, 98 atom%) was injected into the sediment through the lateral silicon ports using a glass syringe (Hamilton 725RN 250 µl, ga 22S/51 mm/pst 2). The volume of $^{15}NH_4^+$ solution added to each microcosm was adjusted to enrich the natural NH_4^+ pool by 30%. During incubations, plants were submerged in a well-mixed tank kept at in situ temperature. At the beginning of the incubation, all the liners were closed with a bottom stopper and a top lid. After 4 hr of incubation, 2 ml of 7 mol/L $ZnCl_2$ was added to the water phase in all the core liners to stop biological activity and the sediment and water phase was gently slurred. A subsample of slurry was collected and transferred into 12-ml exetainers spiked with 200 µl of 7 mol/L $ZnCl_2$. $^{14}N^{15}N$ and $^{15}N^{15}N$ abundance in N_2 was analysed by Membrane Inlet Mass Spectrometry (MIMS, Bay Instrument, USA). The subsurface denitrification (which refers to the denitrification coupled to nitrification occurring within the rhizosphere, below the oxygen penetration depth) was calculated as the sum of D_{15} and D_{14} (which are the rates of denitrification of $^{15}NO_3^-$ and $^{14}NO_3^-$ produced within the sediments via oxidation $^{15}NH_4^+$ and $^{14}NH_4^+$, respectively), according to Risgaard-Petersen and Jensen (1997) and Risgaard-Petersen et al. (1998) and the assumptions of Nielsen (1992).

2.7 | Microplates for 2D ammonium and phosphate distribution in the rhizosphere

The pore water concentration of NH_4^+ and PO_4^{3-} in the rhizosphere was investigated by a modified version of a two-dimensional sampler originally described by Lewandowski, Ruter, and Hupfer (2002). Two polystyrene microplates (Sarstedt, Nubrecht, Germany) were assembled on the opposite sides of an acrylic chamber leaving a narrow space (5 mm) hosting the sediment and the roots. Each microplate consisted of 96 wells with an opening diameter of 6.9 mm (volume 385 µl), arranged in eight rows and 12 columns. The wells were initially filled with O_2-free distilled water and covered by a membrane made from Spectra/por 1 dialysis membrane (Spectrum™) consisting of regenerated cellulose with a molecular weight cut off of 6–8 kDa (Mura et al., 1996). The sediment and the plant were added to the chamber, which was placed in a tank containing aerated in situ water for 14 days. The microplates were then retrieved from the chamber, the membrane was removed and the water from each well sampled for chemical analyses. Soluble reactive phosphorus (i.e. PO_4^{3-}) and NH_4^+ were determined using standard colorimetric methods (Bower & HolmHansen, 1980; Valderrama, 1977) and analysed spectrophotometrically (iMark™ Microplate Absorbance Reader).

2.8 | Environmental scanning electron microscopy imaging on old and new roots and elemental composition of plaques

Presence and elemental spectra of the precipitates on the roots surface were analysed on new and old roots of *V. spiralis* by environmental scanning electron microscope (ESEM) coupled with energy dispersive X-ray spectrometer. Specimens of *V. spiralis* were gently extracted from the sediment and rinsed with in situ water to remove sediment. Sections of new, light-coloured and old, red–dark-coloured roots (5 mm in length) were excised with a sterile scalpel at different depths. Root sections were mounted on aluminium stubs of

Plant		Sediment	
Number of leaves	8	Porosity	0.78 (±0.04, *n* = 3)
Leaves dry weight (g)	0.386	LOI	11%
Roots dry weight (g)	0.096	O_2 pen. depth (mm)	5.2 (±0.05, *n* = 5)
Average root diameter (mm)	0.37 (±0.02, *n* = 6)	R_{SWI} (μmol m^{-2} h^{-1})	234 (±33, *n* = 5)
ROL (μmol m^{-2} h^{-1})	324 (±107, *n* = 6)	R_S (nmol cm^{-3} h^{-1})	96.5 (±15, *n* = 5)

TABLE 1 Characteristic of the plant and sediment. Values reported as mean (±*SEM*). Radial oxygen loss (ROL), Oxygen penetration depth, volumetric O_2 respiration at the sediment surface (R_{SWI}) and at depth (R_S) refer to the treatment with overlying water at 100% air saturation under light conditions

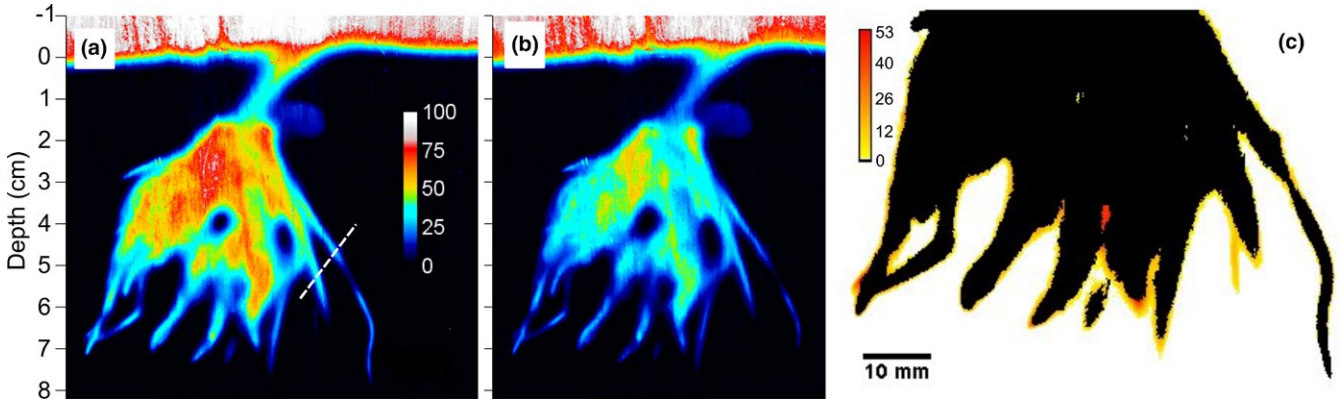

FIGURE 1 Oxygen distribution in the rhizosphere of *V. spiralis*, with ambient water at 100% air saturation (AS) during light (a) and dark (b) periods. Zero on the X-axes indicates the approximate sediment surface. Air saturation level is denoted by colour. White dotted line in (a) shows the transect analysed for comparing ROL in old vs. new roots in Figure 2. Panel (c) shows the areas of the rhizosphere that experience transition between oxic and anoxic (<2 μmol/L O_2) condition during a light–dark cycle with overlying water at 100% AS. Intensity of the fluctuation in O_2 concentrations is indicated by colour and expressed in μmol/L. Black areas indicate zones that are above the 2 μmol/L threshold even during the dark phase

12 mm with double-sided adhesive carbon tape. The prepared samples were then directly analysed at the ESEM (QuantaTM 250 FEG, FEI, Hillsboro, OR, USA) at 15.0 kV, operating in wet mode (room internal relative moisture 100%, temperature 3–5°C and pressure 600–700 Pa).

3 | RESULTS

3.1 | Radial oxygen loss at overlying water at air saturation

The sediment not influenced by the plant had an O_2 penetration of 5.2 ± 0.05 (*SEM*, *n* = 5) mm (Table 1) at 100% air-saturation. The derived O_2 consumption within the top oxic layer of the sediment was 234 ± 33 (*SEM*, *n* = 5) μmol m^{-3} hr^{-1}. In the presence of the rhizosphere, ROL was observed along all visible root segments, with higher O_2 concentrations measured in the top, root-dense part of rhizosphere (Figure 1a). During the light phase, O_2 saturation reached 75% at about 3 cm depth and 25% at about 7 cm depth, in proximity of the root tips. After the onset of darkness, the O_2 availability decreased for a period of 2.5 hr before a new steady-state O_2 distribution was established (see also Video S1 in supporting information). Under these conditions, the prevailing O_2 saturation in the top part of the rhizosphere was 20–40%, with a maximum at 50%. At about 7 cm depth, maximum O_2 saturation

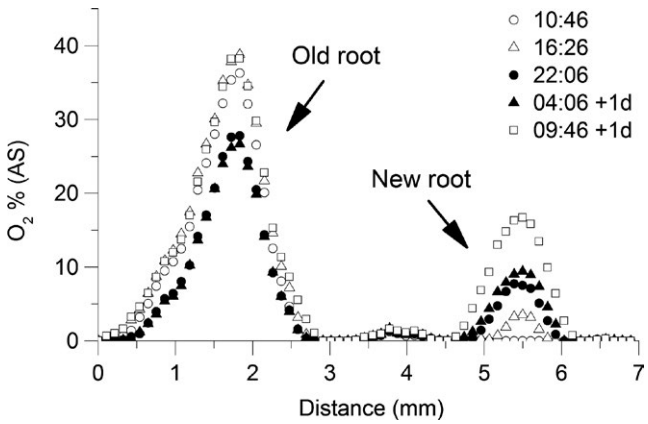

FIGURE 2 Oxygen levels along a transect crossing an old, not growing and a new, growing root. Measurements were repeated over a 24-hr during a light-dark-light cycle. Empty and full symbols indicate measurements time (hr:min) during light and dark conditions, respectively. The location of the transect is illustrated in Figure 1a

decreased to 15% and some of the oxic areas at the root tips turned anoxic (Figure 1b).

The comparative analysis of the light and dark phase images highlighted areas of the rhizosphere where condition shifted from oxic to anoxic levels during one diel cycle (Figure 1c). Ninety-two percent of the

rhizosphere (defined as maximum extent of the oxic area) remained oxic at all time, whilst 8% fluctuated between oxia and anoxia (Table 2). This corresponded to 41.3 cm^3 of sediment remaining oxic and 5.5 cm^3 that oscillated between oxic and anoxic condition. Such fluctuating areas were preferentially located at the peripheral zones of the rhizosphere. Ninety-four percent of such areas fluctuated between anoxia and ≤20 μmol/L O_2, with a mode variation value of 2 μmol/L (Figure S2). The maximum diel amplitude of oxic-anoxic oscillations (50 μmol/L O_2) was found where roots overlaid (Figure 1c). Under light conditions, ROL per root surface area estimated across six roots ranged between 58 and 658 μmol m^{-2} hr^{-1}, with an average value of 324 ± 107 (mean ± *SEM*) μmol m^{-2} hr^{-1}.

3.2 | Radial oxygen loss in old versus new roots

Oxygen transects across an old, not growing root (not increasing in diameter nor in length throughout a light period) and one new, growing root during subsequent light, dark, and light phases are shown in Figure 2. At steady state in light (16:26, hr:min), ROL by the old root led to stable O_2 saturation up to 39%. Oxygen was measured around the root over an area of 2.7 mm in diameter. During the following dark phase, maximum O_2 saturation decreased to 28% and the diameter of the area of net O_2 accumulation contracted to 2.4 mm. Subsequent O_2 saturation remained constant. With the next light phase, O_2 saturation realigned with the values of the previous light phase. No O_2 was measured in the sediment before the appearance of the new growing root (new root, time: 10:46). Net O_2 accumulation (maximum 3.5% O_2 saturation) was measured at 16:36 over an area with a diameter of 1.2 mm. At the first dark measurement (22:06), the maximum O_2 saturation had increased to 7.7% and the oxic area spanned over 1.4 mm. At 4:06, maximum O_2 saturation reached 9.4% with no substantial increase of the oxic diameter. The following measurement with light showed an increase of the O_2 saturation (maximum 17%) and of the oxic area diameter (1.7 mm). Similar dynamics, i.e. retreat of the oxic area during dark period in old roots versus continuous expansion of the oxic areas in new roots, was observed in four additional roots (two old roots and two new roots) (Figure S3).

3.3 | Effect of changing O_2 saturation in the overlying water

Figure 3 shows the variation of the average O_2 saturation within the rhizosphere as a function of O_2 saturation in the overlying water during light/dark periods. During light phases, under 100% O_2 saturation in the water column, the average O_2 saturation in the rhizosphere remained at 34% ± 0.2 (mean ± *SD*; Figure 3b). Oxygen saturation rapidly declined after the onset of darkness. Within 2 hr 20 min, the average O_2 saturation stabilised at 22% ± 0.2 AS. Eighty-five percent of this decline was reached within the first 20 min. Under 38% O_2 saturation in the water column, the average Oxygen in the rhizosphere dropped to 15% ± 0.2 during the light phase and to 4.2% ± 0.1 during the dark phase. Re-increasing the ambient O_2 saturation to 70% increased of the average O_2 saturation of the rhizosphere to 27% ± 0.1 during the light phase, and to 13% ± 0.1 during the dark phase. Overall, the average steady state O_2 saturation in the rhizosphere decreased linearly with the ambient O_2 level of the overlying water under both light and dark conditions (light phase: rhizosphere O_2 saturation = 0.29 × ambient water O_2 saturation + 5.0, r^2 = 0.98; dark phase: rhizosphere O_2 saturation = 0.29 × ambient water O_2 saturation − 6.9; r^2 = 0.99).

Similarly to the average O_2 saturation in the rhizosphere, the extension of the oxic area on the planar optode wall responded to the changes in ambient O_2 saturation and light condition (Table 2). The extension of the oxic area spanned from a maximum 25 cm^2 at 100% O_2 saturation in overlying water during light phase to a minimum of 8.6 cm^2 with overlying water at 38% O_2 saturation during the dark phase. Estimated total O_2 transport via ROL during the light (13 hr) and dark (11 hr) phases was 53.5 and 39.0 μmol, respectively, at 100% O_2 saturation, and 29.8 and 10.4 μmol, respectively, with water at 38% O_2 saturation.

3.4 | Effect of the rhizosphere on sediment denitrification coupled to nitrification

Rates of subsurface denitrification coupled to nitrification in vegetated sediment were about 6 and 2.5-fold higher compared to unvegetated sediment exposed to light and darkness, respectively (Figure 4). In light exposed vegetated sediment, the subsurface denitrification coupled to nitrification (85 ± 10 μmol $N\text{-}N_2$ m^{-2} hr^{-1}, mean ± *SEM*, *n* = 6) was almost twice the values in darkness (45 ± 3 μmol $N\text{-}N_2$ m^{-2} hr^{-1}, mean ± *SEM*, *n* = 6). Rates of subsurface denitrification coupled to nitrification measured in the unvegetated sediment indicate that some $^{15}NH_4^+$ reached the oxic portion of the sediment, but rates remained largely unaffected by light (i.e. 15 ± 2 and 20 ± 2 μmol $N\text{-}N_2$ m^{-2} hr^{-1} under light and dark conditions, respectively).

TABLE 2 Average O_2 level (AS %) in the rhizosphere, extension of the oxic area, extension of the oxic volume, radial oxygen loss (ROL) as O_2 flux by the whole plant under different experimental conditions at steady-state, and integrated O_2 transport via ROL during the whole light and dark phases

	100% (AS)		70% (AS)		38% (AS)	
	Dark	Light	Dark	Light	Dark	Light
Mean O_2 saturation (% AS)	22.2	33.5	13.0	27.0	4.2	15.4
Area (cm^2)	22.9	24.9	17.0	20.8	8.6	17.4
Volume (cm^3)	41.3	46.8	26.3	35.7	9.5	27.2
ROL (μmol h^{-1} $plant^{-1}$)	3.7	4.2	2.3	3.2	0.9	2.4
O_2 transport (μmol/plant)	39.0	53.5	25.3	37.5	1	29.8

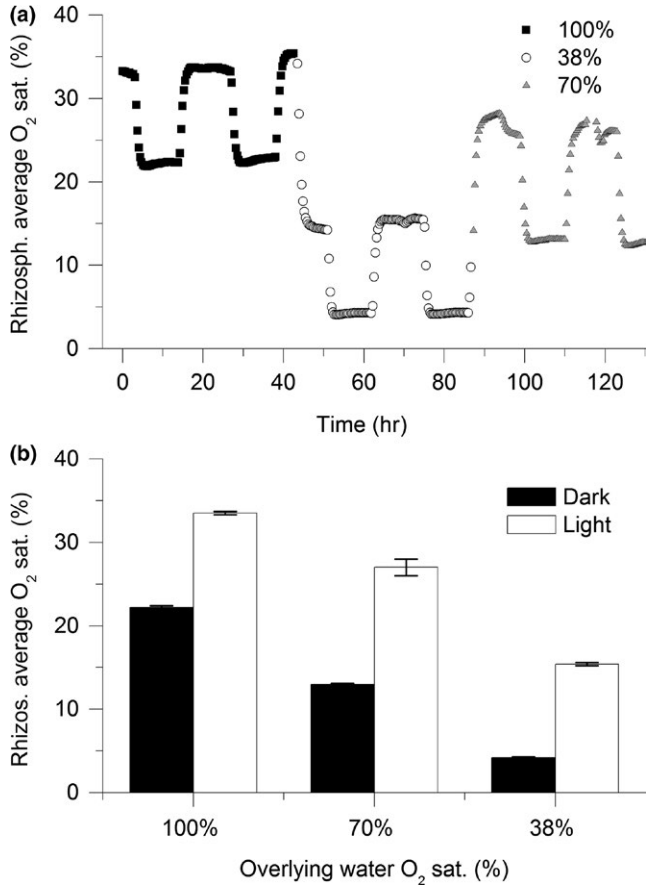

FIGURE 3 Variation of the oxic level in the rhizosphere (defined as the maximum expansion of the oxic area at O_2 level at 100% air saturation in light) under repeated light and dark cycles, at three ambient O_2 levels (as % of air saturation) (a). Average O_2 level (as % of air saturation) in the rhizosphere at quasi steady-state under the various conditions (b)

3.5 | Nutrient availability in the rhizosphere as resolved by the microplate approach

The prevailing NH_4^+ concentration within the rhizosphere was around 15 μmol/L (Figure 5) while concentration in root-free areas reached over 100 μmol/L. Similarly, the phosphate concentration in the basal root zone amounted to 7.6 μmol/L while values increased to about 200 μmol/L in the periphery of the image. Thus, nutrient availability in the rhizosphere was almost one order of magnitude lower than in zones with no roots. Two additional peripheral areas with no apparent link with the rhizosphere (at the sediment surface and at 8 cm depth) also appeared highly PO_4^{3-} depleted (0–6 μmol/L).

3.6 | ESEM imaging on old and new roots and elemental composition of plaques

New roots of *V. spiralis* appeared light-coloured and were clearly distinguishable from old, red–dark-coloured roots (Figure 6b). The red–dark colour was associated with the formation of dense metal plaques as shown by ESEM imaging (Figure 6c). By contrast, new, light-coloured roots appeared bare, with only limited metal plaque precipitation (Figure 6a). Comparative analysis of the elemental composition of the surface of the bare roots and plaque covered roots by energy dispersive X-ray spectrometer revealed a relative enrichment of Fe on the plaques surface (27.0%) compared to the bare root (2.5%; Figure 6d,e); similarly, the P content was higher in the plaques (7.5%) than in the bare roots (1.2%).

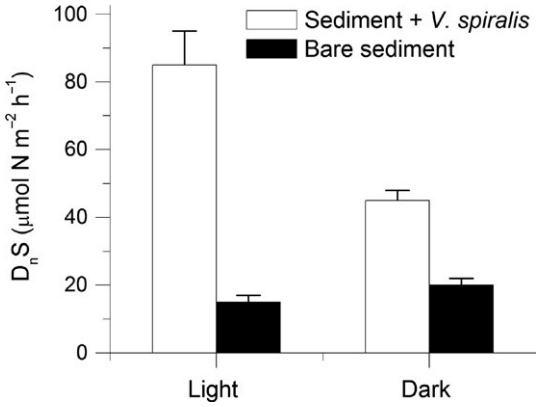

FIGURE 4 Light and dark fluxes of denitrification coupled to nitrification in the subsurface sediment (Dn-S) measured in microcosms with and without *V. spiralis* (mean ± *SEM*, *n* = 6)

4 | DISCUSSION

4.1 | Importance of ROL from *V. spiralis* for benthic O_2 consumption

To our knowledge, the work of Han et al. (2016) and the present study provided the first direct estimates of ROL in *V. spiralis* under conditions close to those met in situ. Rates of ROL from single roots in our study (range, 58.3–658 μmol m^{-2} hr^{-1}) are comparable to rates measured in rice plants (*Oryza sativa*) i.e. 19.2–441 μmol m^{-2} hr^{-1} (Larsen, Santner, Oburger, Wenzel, & Glud, 2015), which are among the highest rates reported in the literature (Han et al., 2016 and references therein). Rates of ROL from single roots of *V. spiralis* measured by Han et al. (2016) via planar optode imaging ranged between 32 and 109 μmol m^{-2} hr^{-1}. Despite the difference in ROL from single roots between the two available studies on *V. spiralis*, our total ROL rate normalised for the root biomass (calculated from total ROL/whole roots dry weight) i.e. 9.5–10.8 μmol O_2 g_{DW} $root^{-1}$ hr^{-1} were similar to the one reported by Han et al. (2016) i.e. 5.2–7.7 μmol O_2 g_{DW} $root^{-1}$ hr^{-1}. This convergence could be linked to a larger fraction of root segments that do not facilitate or have limited ROL in our study. In chemically reduced sediments, ROL facilitates the re-oxidation of Fe^{2+} and its precipitation as iron plaques on the root surface (Povidisa et al., 2009 and references therein). Such plaques can decrease the gas permeability of the roots and thus the ROL (Kaj Sand-Jensen, Møller, & Raun, 2008). Extensive Fe coating was observed in our study on old roots of *V. spiralis* (Figure 6 and later discussion). It is thus plausible that precipitation of Fe oxides has limited ROL in a substantial fraction of the rhizosphere.

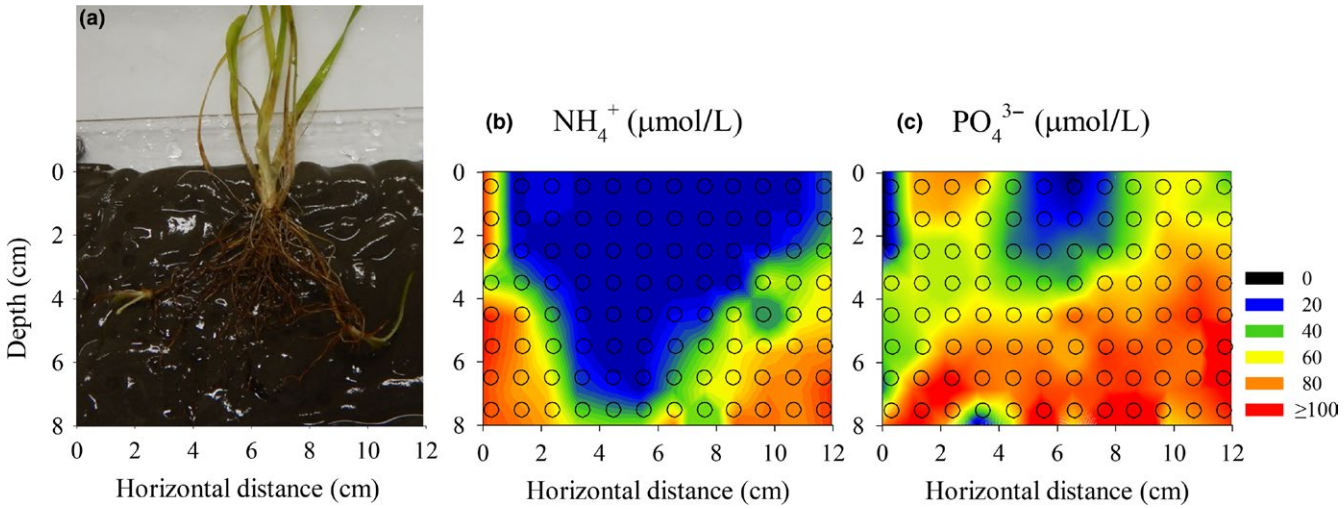

FIGURE 5 Two-dimensional NH_4^+ (b) and PO_4^{3-} (c) isoconcentration diagrams of the rhizosphere sediment obtained by a microplate sampler. Black circles indicate the opening of each sampling well. Panel (a) shows the sediment portion that was analysed before the application of the microplates

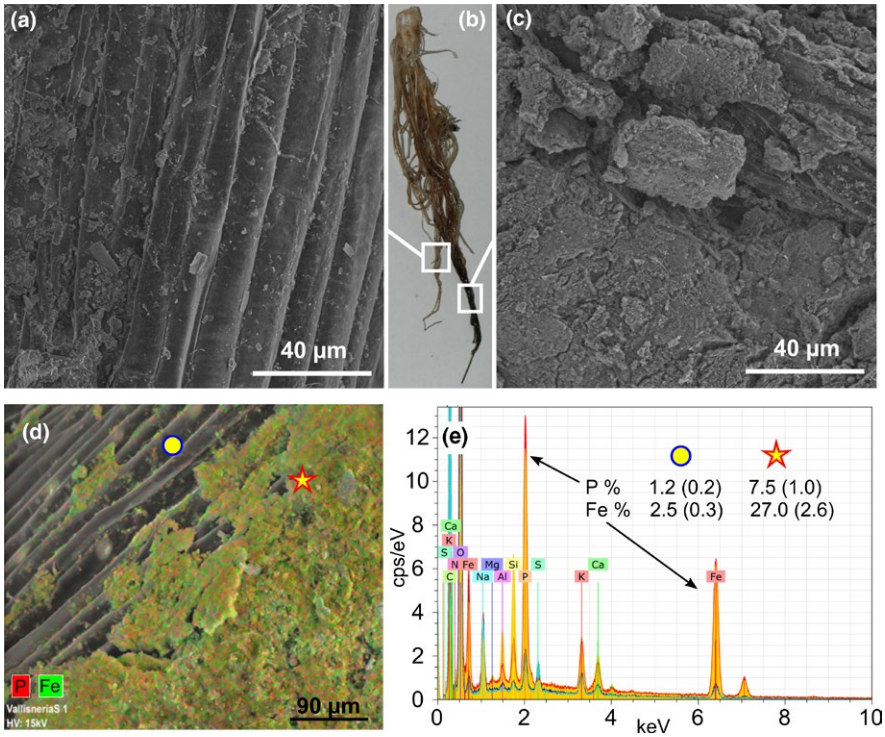

FIGURE 6 Environmental scanning electron microscopy (ESEM) images of young (a) and old (c) roots of *V. spiralis* (b) showing light and heavy plaques formation, respectively. ESEM-coupled to Energy Dispersive X-ray Spectrometer (EDS) image of root surface partially coated by Fe-P plaques (d). EDS spectrum showing elemental composition measured on the bare root (circle) and on the plaque (star) (e). Relative enrichment (weight %) of Fe and P is reported on the panel. Numbers within brackets indicate 3×*SD*

In *V. spiralis*, the O_2 release via ROL occurs all along the root length. This results in a conspicuous transport of O_2 into the rhizosphere as compared to other submerged macrophytes where ROL occurs in partial section of the roots or solely at the root tips e.g. *Zoostera sp.* (*marina and muelleri*) and *Ruppia maritima* (Brodersen, Nielsen, Ralph, & Kuhl, 2015; Jensen et al., 2005; Jovanovic et al., 2015; Koren, Brodersen, Jakobsen, & Kuhl, 2015). Based on the obtained O_2 images, we estimated that one plant of *V. spiralis* increases the total oxic volume of the sediment 447 and 394 times during the day and night, respectively. Considering the ROL of a single plant (as reported in Table 2) and a minimum shoot density of 600 plant/m^2 (Ribaudo et al., 2011), the colonisation of *V. spiralis* can enhance the total O_2 transport into the sediment from to 234 µmol m^{-2} hr^{-1} to 2500 and 2200 µmol m^{-2} hr^{-1} during day and night, respectively. On a daily basis, the ROL by the meadow (56.1 mmol O_2 m^{-2} d^{-1}) can thus increase the sediment respiration (R_{SWI} 5.6 mmol O_2 m^{-2} d^{-1}) by *c.* 10 times. This is substantially higher to what previously reported from marine meadows of *Zoostera m.*, where ROL (2.16–2.48 mmol O_2 m^{-2} d^{-1}) was estimated to accounted only for the 2–14% of the sediment respiration (Frederiksen & Glud, 2006; Jensen et al., 2005), and almost comparable to rice plants with highly gas permeable rhizospheres where ROL (9.9–24.8 mmol O_2 m^{-2} d^{-1}) was 144% of the sediment respiration (Larsen et al., 2015).

4.2 | Control of light and oxic level of the overlying water on ROL

The oxic conditions in the rhizosphere exhibited considerable spatio-temporal variations. At the light-dark shift, the basal root zone of the rhizosphere remained oxic, whereas peripheral areas changed from oxia to anoxia with more pronounced anoxic/oxic oscillations detected where roots intersected. At the single root level, the oxic halo around the non-growing roots expanded and contracted regularly in response to light-dark and dark-light shifts, respectively. In contrast, for growing roots, the oxic halo kept expanding even during darkness (although at slower rates as compared to light conditions). The marginal expansion of the halo between the two successive dark measurements could have been determined by the widening of the root diameter (the root was observed to elongate overnight), or by a possible reduced sediment respiration linked with a lower release of roots exudates in the sediment at darkness (Watt & Evans, 1999). Overall, our data indicate that the rhizosphere hosts a complex mosaic of microenvironments (microbial niches) created by light shifts, root age, assemblage and geometry. This could have important implications for plant performance and the biogeochemical function of the sediment (see later discussion).

In addition, our data show the relative importance of the O_2 saturation of the ambient water versus photosynthesis (at light saturation) in controlling ROL in *V. spiralis*. As reported for other submerged macrophytes, photosynthesis increases the O_2 partial pressure in the aerenchyma, which enhances the ROL (e.g. Pedersen, Borum, Duarte, & Fortes, 1998; Sand-Jensen, Prahl, & Stokholm, 1982). In contrast, during darkness, only the O_2 gradient between the overlying water and the sediment drives the ROL. Thus, the ratio between dark and light values indicates the contribution of the O_2 gradient to the total ROL. With ambient water at 100% and 70% O_2 saturation, the ratios between dark and light values were 0.88 and 0.73, respectively, indicating that the O_2 gradient was the main driver for ROL. At 38% O_2 saturation, the ratio lowered to 0.25 indicating that photosynthesis became more important for driving ROL at severely depleted O_2 levels. With water at 100% O_2 saturation, the ratio calculated for *R. maritima* and *Z. marina*, was approximately 0.4, indicating a relatively lower contribution of the water-sediment gradient to ROL (Jovanovic et al., 2015). The same ratio calculated from ROL estimated from single roots of *Z. marina*, (Frederiksen & Glud, 2006; Jensen et al., 2005) and *Cymodocea rotundata* (Pedersen et al., 1998), generally ranged between 0.39 to 0.45. Although this comparison is based on a limited amount of data, the available studies suggest a more effective transport of O_2 by *V. spiralis* in the sediment in absence of photosynthesis. The maintenance of elevated ROL during darkness by *V. spiralis* is presumably important for colonisation and growth in O_2 depleted eutrophic freshwater characterised by chemically reduced sediment.

In our experiment, (1) the linear correlation between oxic level of the overlying water and ROL intensity, (2) the fast establishment of new steady oxic level in the rhizosphere in response to changing O_2 in the overlying water, and (3) the reversibility of such response, suggest that the variation of ROL is a passive response to the alterations of the O_2 level in the ambient water. The linear relationship between oxic level of the water and ROL also indicates that no or only marginal parts of the rhizosphere will remain oxic in darkness below 30% O_2 saturation in the overlying water (average rhizosphere O_2 saturation about 2%). It remains to be investigated if anatomic adaptation such as variation of root porosity (Lemoine, Mermillod-Blondin, Barrat-Segretain, Masse, & Malet, 2012) or size of the aerenchyma (Colmer, 2003b; Cronk & Fennessy, 2016) could happen to further enhance ROL efficiency in plants exposed to lower O_2 saturations and during longer exposure times than applied in the present study.

4.3 | Spatio-temporal heterogeneity of ROL and implications for N and P cycling

The two-dimensional analysis of NH_4^+ and PO_4^{3-} document an overall nutrient depletion in the rhizosphere, likely due to macrophyte uptake and ROL-dependent processes. For nitrogen, the presence of plants clearly enhanced the denitrification as ROL stimulated subsurface nitrification – particularly during the day time. The plants thereby facilitated microbial driven removal of bioavailable nitrogen. This observation is consistent with previous data reported by Soana et al. (2015) and Racchetti et al. (2017). In bio-irrigated sediments, the mobilisation of N species (enhanced release of NH_4^+ in anoxic phase, enhanced nitrification in the oxic phase, and overall simulation of denitrification activity) is known to be favoured under oscillating redox conditions (Gilbert, Hulth, Grossi, & Aller, 2016). Similar dynamics could occur in the rhizosphere of *V. spiralis* in response to day and night shifts. In particular, pronounced redox oscillations are expected to occur in the peripheral areas where conditions shift from oxic to anoxic on a daily basis. In these areas, the activity of nitrifying microorganisms can also be stimulated by a higher availability of NH_4^+ compared to the root-dense, NH_4^+-depleted core of the rhizosphere where nitrification may face more intense competition with plant uptake (see later discussion). From the linear regression between ambient water O_2 level and oxic area of the rhizosphere, it can be estimated that a variation of ambient water O_2 saturation of 15% will result in the oscillation of the oxic area of the rhizosphere similar to the one observed at light/dark shifts with ambient water at 100% O_2 saturation (i.e. contraction of the oxic area of 2 cm^2). This suggests that an effect on the rhizosphere N dynamics similar to the one induced by day/night shift can also be expected from moderate variations in ambient water O_2 level. All in all, our data indicate that the rapid (hours to days) modulation of ROL in response to variation in light regime and possibly in ambient water O_2 concentration can directly influence microbial-driven N transformations and overall enhance the ability of the rhizosphere to work as a N sink in the riverbed.

The variation of NH_4^+ concentration in the rhizosphere is ultimately determined by the balance between consumption processes (i.e. plant uptake and bacterial nitrification), and supply via organic matter decomposition (ammonification). Theoretical N uptake by *V. spiralis*, estimated for plants from the same site ranged

between 380 and 680 μm m^{-2} hr^{-1} in spring and between 6,600 and 10,000 μm m^{-2} hr^{-1} in summer months (Racchetti et al., 2017). These values are one to three orders of magnitude higher compared to our data on subsurface denitrification coupled to nitrification activity (45–85 μm m^{-2} hr^{-1}). Uptake, more than nitrification, seems thus to drive the consumption of NH_4^+ in the rhizosphere, unless NO_3^- uptake from the water column is significant. A maximum rate of ammonification in the rhizosphere can be estimated from the O_2 consumption rate of the vegetated sediment (assuming a respiratory coefficient O_2:C = 1) and the sediment C:N ratio (i.e. 23 from Soana et al., 2015). The thereby calculated rate of ammonification (i.e. 109 μmol m^{-2} hr^{-1}) is substantially lower than the sum of the NH_4^+ consuming processes. The mismatch between consumption and supply can thus explain the NH_4^+ depletion in the rhizosphere observed in our study.

Phosphate was also highly depleted in the rhizosphere. Similarly to NH_4^+, net PO_4^{3-} depletion is probably linked with potential P production in the sediment much lower than P uptake. Our data show that in addition to plant uptake, P-enriched Fe-plaques on root of *V. spiralis* can also act as PO_4^{3-} sink. The formation of Fe plaques on the roots surface results from the precipitation of pore water-dissolved ferrous iron as insoluble Fe(III) oxides–hydroxides at the higher redox potential induced by ROL (e.g. Bacha & Hossner, 1977). Conversely, under prevailing anoxic conditions lower redox potential may favour the dissolution of Fe(III) oxides–hydroxides with consequent liberation PO_4^{3-} (Azzoni, Giordani, Bartoli, Welsh, & Viaroli, 2001; Racchetti et al., 2010). Sedimentary Pools can thus be made available during oxic-anoxic shifts. However, a recent publication (Han et al., 2018) suggests that P daily variations are much lower than those of O_2, leaving space for further studies targeting how plants exploit sedimentary nutrients. The immobilisation of P in Fe-plaques as induced by ROL is in apparent contrast with the need of the plant to take up dissolved P (Christensen & Sand-Jensen, 1998). To overcome this possible limitation, recent studies showed that aquatic plants can *re-gain* P from plaques by promoting their dissolution (via stimulating acid production or Fe III reduction) for assimilation purposes (Brodersen et al., 2017; Xing et al., 2018). Our O_2 and environmental scanning electron microscopy coupled with energy dispersive X-ray spectrometer data show that conditions favouring precipitation or dissolution of Fe-P plaques coexist in the rhizosphere and that such heterogeneity persists at both macro- and micro-scales. Maintaining high spatial and temporal heterogeneity of chemical niches could thus represent a mechanisms per se to both accumulate (in plaques) and mobilise (in transiently or permanently reduced areas of the rhizosphere) P, which has low concentrations in the water column and is generally assimilated from the sediment.

ACKNOWLEDGMENTS

This study was financially supported by a research grant *Blokstipendium* from the Villum Foundation awarded to RNG (13881). Furthermore, the study was financially supported by European Union's Horizon 2020 research and innovation programme, (HADES-ERC grant agreement No 669947) RNG; and The Danish National Research Council (FNU; 0602-02276B; 12-125843) RNG.

ORCID

Ugo Marzocchi https://orcid.org/0000-0002-4746-9944
Sara Benelli https://orcid.org/0000-0002-1684-4609

REFERENCES

Armstrong, W. (1979). Aeration in higher plants. In H. W. Woolhouse (Ed.), *Advances in botanical research* (Vol. 7, pp. 225–332). London, UK: Academic Press.

Azzoni, R., Giordani, G., Bartoli, M., Welsh, D. T., & Viaroli, P. (2001). Iron, sulphur and phosphorus cycling in the rhizosphere sediments of a eutrophic *Ruppia cirrhosa* meadow (Valle Smarlacca, Italy). *Journal of Sea Research*, *45*(), 15–26. https://doi.org/10.1016/s1385-1101(00)00056-3

Bacha, R. E., & Hossner, L. R. (1977). Characteristics of coatings formed on rice roots as affected by iron and manganese additions. *Soil Science Society of America Journal*, *41*, 931–935. https://doi.org/10.2136/sssaj1977.03615995004100050025x

Berg, P., Risgaard-Petersen, N., & Rysgaard, S. (1998). Interpretation of measured concentration profiles in sediment pore water. *Limnology and Oceanography*, *43*, 1500–1510. https://doi.org/10.4319/lo.1998.43.7.1500

Boudreau, B. D. (1997). *Diagenetic models and their implementation*. Berlin, Germany: Springer-Verlag. https://doi.org/10.1007/978-3-642-60421-8

Bower, C. E., & HolmHansen, T. (1980). A salicylate-hypochlorite method for determining ammonia in seawater. *Canadian Journal of Fisheries and Aquatic Sciences*, *37*, 794–798. https://doi.org/10.1139/f80-106

Brodersen, K. E., Koren, K., Mosshammer, M., Ralph, P. J., Kuhl, M., & Santner, J. (2017). Seagrass-mediated phosphorus and iron solubilization in tropical sediments. *Environmental Science & Technology*, *51*, 14155–14163. https://doi.org/10.1021/acs.est.7b03878

Brodersen, K. E., Nielsen, D. A., Ralph, P. J., & Kuhl, M. (2015). Oxic microshield and local pH enhancement protects *Zostera muelleri* from sediment derived hydrogen sulphide. *New Phytologist*, *205*, 1264–1276. https://doi.org/10.1111/nph.13124

Caffrey, J. M., & Kemp, W. M. (1991). Seasonal and spatial patterns of oxygen production, respiration and root rhizome release in Potamogeton-Perfoliatus L and Zostera-Marina L. *Aquatic Botany*, *40*, 109–128. https://doi.org/doi 10.1016/0304-3770(91)90090-R

Christensen, K. K., Jensen, H. S., Andersen, F. O., Wigand, C., & Holmer, M. (1998). Interferences between root plaque formation and phosphorus availability for isoetids in sediments of oligotrophic lakes. *Biogeochemistry*, *43*, 107–128. https://doi.org/doi 10.1023/A:1006010502422

Christensen, K. K., & Sand-Jensen, K. (1998). Precipitated iron and manganese plaques restrict root uptake of phosphorus in *Lobelia dortmanna*. *Canadian Journal of Botany-Revue Canadienne De Botanique*, *76*, 2158–2163. https://doi.org/10.1139/b98-181

Colmer, T. D. (2003a). Aerenchyma and an inducible barrier to radial oxygen loss facilitate root aeration in upland, paddy and deep-water rice (*Oryza sativa* L.). *Annals of Botany*, *91*, 301–309. https://doi.org/10.1093/aob/mcf114

Colmer, T. D. (2003b). Long-distance transport of gases in plants: A perspective on internal aeration and radial oxygen loss from roots. *Plant Cell and Environment*, *26*, 17–36. https://doi.org/10.1046/j.1365-3040.2003.00846.x

Cronk, J. K., & Fennessy, M. S. (2016). *Adaptations to growth conditions in wetlands Wetland plants: Biology and ecology* (pp. 87–146). CRC Press.

Dalsgaard, T., Nielsen, L. P., Brotas, V., Viaroli, P., Underwood, G., Nedwell, D. B., … Risgaard-Pedersen, N. (2000). *Protocol handbook for NICE - Nitrogen Cycling in Estuaries: a project under the EU research programme: Marine Science and Technology (MAST III)*(pp. 62). Silkeborg, Denmark: National Environmental Research Institute.

Fenchel, T. (1996). Worm burrows and oxic microniches in marine sediments. 1. Spatial and temporal scales. *Marine Biology*, *127*, 289–295. https://doi.org/10.1007/bf00942114

Frederiksen, M. S., & Glud, R. N. (2006). Oxygen dynamics in the rhizosphere of *Zostera marina*: A two-dimensional planar optode study. *Limnology and Oceanography*, *51*, 1072–1083. https://doi.org/10.4319/lo.2006.51.2.1072

Geurts, J. J. M., Sarneel, J. M., Willers, B. J. C., Roelofs, J. G. M., Verhoeven, J. T. A., & Lamers, L. P. M. (2009). Interacting effects of sulphate pollution, sulphide toxicity and eutrophication on vegetation development in fens: A mesocosm experiment. *Environmental Pollution*, *157*, 2072–2081. https://doi.org/10.1016/j.envpol.2009.02.024

Gilbert, F., Hulth, S., Grossi, V., & Aller, R. C. (2016). Redox oscillation and benthic nitrogen mineralization within burrowed sediments: An experimental simulation at low frequency. *Journal of Experimental Marine Biology and Ecology*, *482*, 75–84. https://doi.org/10.1016/j.jembe.2016.05.003

Glud, R. N. (2008). Oxygen dynamics of marine sediments. *Marine Biology Research*, *4*, 243–289. https://doi.org/doi 10.1080/17451000801888726

Glud, R. N., Ramsing, N. B., Gundersen, J. K., & Klimant, I. (1996). Planar optrodes: A new tool for fine scale measurements of two-dimensional O-2 distribution in benthic communities. *Marine Ecology Progress Series*, *140*, 217–226. https://doi.org/doi 10.3354/Meps140217

Han, C., Ren, J., Tang, H., Xu, D., & Xie, X. (2016). Quantitative imaging of radial oxygen loss from *Valisneria spiralis* roots with a fluorescent planar optode. *Science of the Total Environment*, *569–570*, 1232–1240. https://doi.org/10.1016/j.scitotenv.2016.06.198

Han, C., Ren, J., Wang, Z., Yang, S., Ke, F., Xu, D., & Xie, X. (2018). Characterization of phosphorus availability in response to radial oxygen losses in the rhizosphere of *Vallisneria spiralis*. *Chemosphere*, *208*, 740–748. https://doi.org/10.1016/j.chemosphere.2018.05.180

Harvey, H. R., Tuttle, J. H., & Bell, J. T. (1995). Kinetics of phytoplankton decay during simulated sedimentation – Changes in biochemical-composition and microbial activity under oxic and anoxic conditions. *Geochimica Et Cosmochimica Acta*, *59*, 3367–3377. https://doi.org/10.1016/0016-7037(95)00217-n

Jensen, S. I., Kuhl, M., Glud, R. N., Jorgensen, L. B., & Prieme, A. (2005). Oxic microzones and radial oxygen loss from roots of *Zostera marina*. *Marine Ecology Progress Series*, *293*, 49–58. https://doi.org/10.3354/meps293049

Jovanovic, Z., Pedersen, M. O., Larsen, M., Kristensen, E., & Glud, R. N. (2015). Rhizosphere O-2 dynamics in young *Zostera marina* and *Ruppia maritima*. *Marine Ecology Progress Series*, *518*, 95–105. https://doi.org/10.3354/meps11041

Klimant, I., Meyer, V., & Kuhl, M. (1995). Fiberoptic oxygen microsensors, a new tool in aquatic biology. *Limnology and Oceanography*, *40*, 1159–1165. https://doi.org/10.4319/lo.1995.40.6.1159

Koch, M. S., & Mendelssohn, I. A. (1989). Sulfide as a soil phytotoxin – Differential responses in 2 marsh species. *Journal of Ecology*, *77*, 565–578. https://doi.org/doi 10.2307/2260770

Koren, K., Brodersen, K. E., Jakobsen, S. L., & Kuhl, M. (2015). Optical sensor nanoparticles in artificial sediments-a new tool to visualize O_2 dynamics around the rhizome and roots of seagrasses. *Environmental Science & Technology*, *49*, 2286–2292. https://doi.org/10.1021/es505734b

Larsen, M., Borisov, S. M., Grunwald, B., Klimant, I., & Glud, R. N. (2011). A simple and inexpensive high resolution color ratiometric planar optode imaging approach: Application to oxygen and pH sensing. *Limnology and Oceanography-Methods*, *9*, 348–360. https://doi.org/10.4319/lom.2011.9.348

Larsen, M., Santner, J., Oburger, E., Wenzel, W. W., & Glud, R. N. (2015). O-2 dynamics in the rhizosphere of young rice plants (*Oryza sativa* L.) as studied by planar optodes. *Plant and Soil*, *390*, 279–292. https://doi.org/10.1007/s11104-015-2382-z

Laskov, C., Horn, O., & Hupfer, M. (2006). Environmental factors regulating the radial oxygen loss from roots of *Myriophyllum spicatum* and *Potamogeton crispus*. *Aquatic Botany*, *84*, 333–340. https://doi.org/10.1016/j.aquabot.2005.12.005

Lemoine, D. G., Mermillod-Blondin, F., Barrat-Segretain, M. H., Masse, C., & Malet, E. (2012). The ability of aquatic macrophytes to increase root porosity and radial oxygen loss determines their resistance to sediment anoxia. *Aquatic Ecology*, *46*, 191–200. https://doi.org/10.1007/s10452-012-9391-2

Lewandowski, J., Ruter, K., & Hupfer, M. (2002). Two-dimensional small-scale variability of pore water phosphate in freshwater lakes: Results from a novel dialysis sampler. *Environmental Science & Technology*, *36*, 2039–2047. https://doi.org/10.1021/es0102538

Longhi, D., Bartoli, M., Nizzoli, D., & Viaroli, P. (2013). Benthic processes in fresh water fluffy sediments undergoing resuspension. *Journal of Limnology*, *72*, 1–12. https://doi.org/10.4081/jlimnol.2013.e1

Magri, M., Benelli, S., Bondavalli, C., Bartoli, M., Christian, R. R., & Bodini, A. (2018). Benthic N pathways in illuminated and bioturbated sediments studied with network analysis. *Limnology and Oceanography*, *63*, S68–S84. https://doi.org/10.1002/lno.10724

Mei, X. Q., Yang, Y., Tam, N. F. Y., Wang, Y. W., & Li, L. (2014). Roles of root porosity, radial oxygen loss, Fe plaque formation on nutrient removal and tolerance of wetland plants to domestic wastewater. *Water Research*, *50*, 147–159. https://doi.org/10.1016/j.watres.2013.12.004

Meysman, F. J. R., Galaktionov, O. S., Glud, R. N., & Middelburg, J. J. (2010). Oxygen penetration around burrows and roots in aquatic sediments. *Journal of Marine Research*, *68*, 309–336. https://doi.org/doi 10.1357/002224010793721406

Mura, M. P., Agusti, S., delGiorgio, P. A., Gasol, J. M., Vaque, D., & Duarte, C. M. (1996). Loss-controlled phytoplankton production in nutrient-poor littoral waters of the NW Mediterranean: In situ experimental evidence. *Marine Ecology Progress Series*, *130*, 213–219. https://doi.org/10.3354/meps130213

Nielsen, L. P. (1992). Denitrification in sediment determined from nitrogen isotope pairing. *Fems Microbiology Ecology*, *86*, 357–362.

Pedersen, O., Borum, J., Duarte, C. M., & Fortes, M. D. (1998). Oxygen dynamics in the rhizosphere of *Cymodocea rotundata*. *Marine Ecology Progress Series*, *169*, 283–288. https://doi.org/10.3354/meps169283

Pinardi, M., Bartoli, M., Longhi, D., Marzocchi, U., Laini, A., Ribaudo, C., & Viaroli, P. (2009). Benthic metabolism and denitrification in a river reach: A comparison between vegetated and bare sediments. *Journal of Limnology*, *68*, 133–145. https://doi.org/10.4081/jlimnol.2009.133

Povidisa, K., Delefosse, M., & Holmer, M. (2009). The formation of iron plaques on roots and rhizomes of the seagrass *Cymodocea serrulata* (R. Brown) Ascherson with implications for sulphide intrusion. *Aquatic Botany*, *90*, 303–308. https://doi.org/10.1016/j.aquabot.2008.11.008

Racchetti, E., Bartoli, M., Ribaudo, C., Longhi, D., Brito, L. E. Q., Naldi, M., … Viaroli, P. (2010). Short term changes in pore water chemistry in river sediments during the early colonization by *Vallisneria spiralis*. *Hydrobiologia*, *652*, 127–137. https://doi.org/10.1007/s10750-010-0324-6

Racchetti, E., Longhi, D., Ribaudo, C., Soana, E., & Bartoli, M. (2017). Nitrogen uptake and coupled nitrification-denitrification in riverine sediments with benthic microalgae and rooted macrophytes. *Aquatic Sciences*, *79*, 487–505. https://doi.org/10.1007/s00027-016-0512-1

Ribaudo, C., Bartoli, M., Racchetti, E., Longhi, D., & Viaroli, P. (2011). Seasonal fluxes of O-2, DIC and CH4 in sediments with *Vallisneria spiralis*: Indications for radial oxygen loss. *Aquatic Botany*, *94*, 134–142. https://doi.org/10.1016/j.aquabot.2011.01.003

Risgaard-Petersen, N., Dalsgaard, T., Rysgaard, S., Christensen, P. B., Borum, J., McGlathery, K., & Nielsen, L. P. (1998). Nitrogen balance of a temperate eelgrass *Zostera marina* bed. *Marine Ecology Progress Series*, *174*, 281–291. https://doi.org/10.3354/meps174281

Risgaard-Petersen, N., & Jensen, K. (1997). Nitrification and denitrification in the rhizosphere of the aquatic macrophyte *Lobelia dortmanna* L. *Limnology and Oceanography*, *42*, 529–537. https://doi.org/10.4319/lo.1997.42.3.0529

Sand-Jensen, K., Møller, C. L., & Raun, A. L. (2008). Outstanding *Lobelia dortmanna* in iron armor. *Plant Signaling & Behavior*, *3*, 882–884. https://doi.org/10.4161/psb.3.10.6500

Sand-Jensen, K., Prahl, C., & Stokholm, H. (1982). Oxygen release from roots of submerged aquatic macrophytes. *Oikos*, *38*, 349–354. https://doi.org/doi 10.2307/3544675

Smirnoff, N., & Crawford, R. M. M. (1983). Variation in the structure and response to flooding of root aerenchyma in some wetland plants. *Annals of Botany*, *51*, 237–249. https://doi.org/10.1093/oxfordjournals.aob.a086462

Soana, E., & Bartoli, M. (2013). Seasonal variation of radial oxygen loss in *Vallisneria spiralis* L.: An adaptive response to sediment redox? *Aquatic Botany*, *104*, 228–232. https://doi.org/10.1016/j.aquabot.2012.07.007

Soana, E., Naldi, M., Bonaglia, S., Racchetti, E., Castaldelli, G., Bruchert, V., … Bartoli, M. (2015). Benthic nitrogen metabolism in a macrophyte meadow (*Vallisneria spiralis* L.) under increasing sedimentary organic matter loads. *Biogeochemistry*, *124*, 387–404. https://doi.org/10.1007/s10533-015-0104-5

St-Cyr, L., Fortin, D., & Campbell, P. G. C. (1993). Microscopic observations of the iron plaque of a submerged aquatic plant (Vallisneria-Americana Michx). *Aquatic Botany*, *46*, 155–167. https://doi.org/doi 10.1016/0304-3770(93)90043-V

Ullman, W. J., & Aller, R. C. (1982). Diffusion-coefficients in nearshore marine-sediments. *Limnology and Oceanography*, *27*, 552–556. https://doi.org/10.4319/lo.1982.27.3.0552

Valderrama, J. C. (1977). Methods used by the hydrographic department of national board of fisheries, Sweden. In K. Grasshoff (Ed.), *Report of the Baltic Intercalibration Workshop* (pp. 14–34). Gothenborg, Sweden: Interim Commission for the Protection of the Environment of the Baltic Sea.

Watt, M., & Evans, J. R. (1999). Linking development and determinacy with organic acid efflux from proteoid roots of white lupin grown with low phosphorus and ambient or elevated atmospheric CO_2 concentration. *Plant Physiology*, *120*, 705–716. https://doi.org/10.1104/pp.120.3.705

Wenzhöfer, F., & Glud, R. N. (2004). Small-scale spatial and temporal variability in coastal benthic O2 dynamics: Effects of fauna activity. *Limnology and Oceanography*, *49*, 1471–1481. https://doi.org/10.4319/lo.2004.49.5.1471

Xing, X. G., Ding, S. M., Liu, L., Chen, M. S., Yan, W. M., Zhao, L. P., & Zhang, C. S. (2018). Direct evidence for the enhanced acquisition of phosphorus in the rhizosphere of aquatic plants: A case study on *Vallisneria natans*. *Science of the Total Environment*, *616*, 386–396. https://doi.org/10.1016/j.scitotenv.2017.10.304

SUPPORTING INFORMATION

Additional supporting information may be found online in the Supporting Information section at the end of the article.

How to cite this article: Marzocchi U, Benelli S, Larsen M, Bartoli M, Glud RN. Spatial heterogeneity and short-term oxygen dynamics in the rhizosphere of *Vallisneria spiralis*: Implications for nutrient cycling. *Freshw Biol*. 2019;64:532–543. https://doi.org/10.1111/fwb.13240